

ASTROPHYSICAL EVIDENCE FOR BLACK HOLE EVENT HORIZONS

K. MENO, E. QUATAERT AND R. NARAYAN
*Harvard-Smithsonian Center for Astrophysics,
 60 Garden Street, Cambridge, MA 02138, USA*

Abstract.¹

Astronomers have discovered many potential black holes in X-ray binaries and galactic nuclei. These black holes are usually identified by the fact that they are too massive to be neutron stars. Until recently, however, there was no convincing evidence that the objects identified as black hole candidates actually have event horizons. This has changed with extensive applications of a class of accretion models for describing the flow of gas onto compact objects; for these solutions, called advection-dominated accretion flows (ADAFs), the black hole nature of the accreting star, specifically its event horizon, plays an important role. We review the evidence that, at low luminosities, accreting black holes in both X-ray binaries and galactic nuclei contain ADAFs rather than the standard thin accretion disk.

1. Introduction

Astronomers have identified potential black holes in a variety of astrophysical objects. In binary star systems, consisting of two stars revolving around each other under the influence of their mutual gravitational attraction, black holes with masses of order several solar masses ($M \sim 5 - 20M_{\odot}$) are thought to exist as the dead remnant of the initially more massive of the two stars.

Occasionally, the black hole in such a system accretes (receives) matter from the outer layers of its companion and the binary becomes a powerful emitter of high energy radiation (hence the name: X-ray binary, XRB) [135]. The radiation is ultimately due to the conversion of gravitational potential

¹To appear also in the Proceedings of The Eighth Marcel Grossmann Meeting.

energy: matter heats up as it falls into the deep potential well of the black hole and the hot gas radiates [38].

In addition, supermassive black holes ($M \sim 10^6 - 10^{10} M_\odot$) probably exist at the centers of most galaxies. By accreting matter (stars or gas) in their vicinity, these black holes may produce the intense emission that we observe from quasars and other Active Galactic Nuclei (AGN) [134].

Since the discovery of black hole solutions in Einstein’s theory of general relativity [100],[61], no definitive proof of their existence has been found. The main issue is that a black hole remains, by its very nature, concealed to the electromagnetic observer and can only be observed through its indirect gravitational influence on the world beyond its event horizon [82]. Mass estimates of compact objects in some systems argue for the existence of black holes. In addition, several observational signatures have been proposed as suggestive of a black hole environment. These lines of evidence do not, however, constitute definitive proof of the reality of black holes.

Recently, a class of accretion solutions called advection-dominated accretion flows (ADAFs) has been extensively applied to a number of accretion systems; for these models, most of the gravitational energy released in the infalling gas is carried (or advected) with the accretion flow as thermal energy, rather than being radiated as in standard solutions [94]. Since a large amount of energy falls onto the central object, there is an important distinction between compact objects with an event horizon and those without; for those with an event horizon, the energy is “lost” to the outside observer after it falls onto the central object, while for those with a hard surface, the energy is re-radiated and ultimately observed [96]. This new and potentially powerful method of discriminating between black holes and other kinds of compact objects is the subject of this review.

In §2, we list the best black hole candidates, and briefly review the classical techniques and theories used to detect potential black holes. In §3, we describe various solutions to the astrophysical problem of gas accreting onto a central object, emphasizing the specific characteristics of ADAFs. In §4, we describe how ADAF models have been applied to X-ray binaries and galactic nuclei and we explain why these studies strengthen the evidence for the existence of black holes.

2. “Classical” Evidence for Black Holes

2.1. EVIDENCE BASED ON MASS IN X-RAY BINARIES

It is well known that neutron stars possess a maximum mass above which they collapse to a black hole. The precise mass limit is not known due to uncertainties in the physics of neutron star interiors; like white dwarfs, neutron stars are supported by degeneracy pressure [16], but unlike white

dwarfs, nuclear forces play an important role in their structure [53]. The equation of state of matter at ultra-nuclear densities is not well known. The maximum mass for the stiffest equation of state is $\sim 3 M_\odot$ [58], and the limit goes up by no more than 25 % if one includes the effects of rotation [39],[123]. Even without detailed knowledge of the equation of state, it is possible from first principles to put a limit on the maximum mass. With an equation of state satisfying causality (sound speed less than the speed of light) and assuming that general relativity is correct, the limit is $\sim 3.4 M_\odot$ [116]. Without causality, it reaches $5.2 M_\odot$ [54],[123]. Although exotic compact stars with very large masses could theoretically exist [4],[81], it is generally accepted by the astronomical community that compact stellar objects with masses above $\sim 3 M_\odot$ are strong black hole candidates.

In various X-ray binary systems, one can constrain the mass of the central object by observations of the spectral lines of the secondary star (usually a main-sequence star). The Doppler shifts of these spectral lines give an estimate of the radial velocity of the secondary relative to the observer. When combined with the orbital period of the binary, this can be translated (through Kepler’s 3rd law) into a “mass function” for the compact object,

$$f(M_X) = \frac{M_X \sin^3 i}{(1 + q)^2}. \quad (1)$$

The mass function does not directly give the mass M_X of the compact star because of its dependence on the unknown inclination i between the normal to the binary orbital plane and the line of sight, and the ratio of the secondary mass to the compact star mass, $q = M_2/M_X$. However, the mass function is a firm lower limit to M_X . Therefore, mass functions above $3 M_\odot$ suggest the presence of black holes. Additional observational data (absence or presence of eclipses, for instance, or information on the nature of the secondary star) can help to constrain i or q , so that a likely value of M_X can often be determined. The best stellar mass black hole candidates currently known are summarized in Table 1. A detailed account of dynamical mass estimates can be found in *X-ray Binaries* [135].

2.2. EVIDENCE BASED ON MASS AND VELOCITY PROFILES OF GALACTIC CENTERS

Lynden-Bell’s conjecture [70] that AGN are powered by accreting super-massive black holes is supported by the intense and energetic emission seen in these systems (implying a high efficiency process like accretion onto a compact object, cf. 3.1). Observations of superluminal jets in some sources (implying a relativistic source) confirm the hypothesis. In addition, rapid variability of the luminosity, in particular the X-ray luminosity, is often

TABLE 1. The best black hole candidates among XRBs [20],[133]. Type refers to Low Mass X-ray Binary (relatively low mass companion star) vs. High Mass X-ray Binary. Mass functions $f(M_X)$ and likely masses M_X are given in solar units (M_\odot).

Object	Type	$f(M_X)$	Likely M_X	References
GRO J0422+32 (XN Per 92)	LMXB	1.21 ± 0.06	≥ 9	[7],[15],[36]
A 0620-00 (XN Mon 75)	LMXB	2.91 ± 0.08	$4.9 - 10$	[72],[120]
GRS 1124-683 (XN Mus 91)	LMXB	3.01 ± 0.15	$5 - 7.5$	[101]
4U 1543-47	LMXB	0.22 ± 0.02	$1.2 - 7.9$	[103]
GRO J1655-40 (XN Sco 94)	LMXB	3.16 ± 0.15	7.02 ± 0.22	[5],[102]
H 1705-250 (XN Oph 77)	LMXB	4 ± 0.8	4.9 ± 1.3	[113]
GS 2000+250 (XN Vul 88)	LMXB	4.97 ± 0.1	8.5 ± 1.5	[14]
GS 2023+338 (V404 Cyg)	LMXB	6.08 ± 0.06	12.3 ± 0.3	[119],[118]
0538-641 (LMC-X-3)	HMXB	2.3 ± 0.3	$7 - 14$	[22]
1956+350 (Cyg X-1)	HMXB	0.24 ± 0.01	$7 - 20$	[46]

observed. For a time-scale of variability Δt , causality implies a source size less than $R \sim c\Delta t$, where c is the speed of light. The estimates of R from the observed variability are typically small, thus supporting the black hole hypothesis [134].

In recent years, new lines of evidence have emerged, thanks to improved observational techniques. Detailed spectroscopic studies of the central regions of nearby galaxies provide valuable information on the line-of-sight velocities of matter (gas or stars). Since the presence of a massive black hole influences the dynamics of matter orbiting around it [10], these studies can help discriminate between black hole and non black hole models. Current results favor the presence of black holes, but alternative scenarios still remain possible [65]. In Table 2 we list the best supermassive black hole candidates revealed by these techniques [117],[37].

2.3. EVIDENCE BASED ON X-RAY SPECTRAL LINES

X-ray emission lines are observed in many Seyfert 1 galaxies (a subclass of AGN). The lines are probably due to fluorescence by iron atoms in a

TABLE 2. Summary of supermassive black hole candidates at the centers of nearby galaxies. The first three are the best candidates. The likely mass is given in solar units (M_\odot).

Galaxy	Likely Mass	References
Milky Way (Sgr A*)	2.5×10^6	[27],[50],[51],[45]
NGC 4486 (M87)	3.2×10^9	[52],[71]
NGC 4258	3.6×10^7	[83]
NGC 224 (M31)	7.5×10^7	[65],[37]
NGC 221 (M32)	3×10^6	[8],[126],[127]
NGC 1068	10^7	[47]
NGC 3115	2×10^9	[62]
NGC 3377	8×10^7	[65]
NGC 3379	$0.5 - 2 \times 10^8$	[42]
NGC 4261	4.9×10^8	[35]
NGC 4342	3.2×10^8	[37]
NGC 4374 (M84)	1.5×10^9	[13]
NGC 4486B	6×10^8	[64]
NGC 4594	10^9	[63]
NGC 4945	10^6	[48]
NGC 6251	7.5×10^8	[37]
MCG-6-30-15	?	[125],[33]

relatively cold gas irradiated by X-ray photons [43],[79]. As matter nears a black hole, the velocity of the gas becomes large. Doppler shifts, as well as gravitational redshifts, are expected in the observed radiation. In the galaxy MCG-6-30-15, a very broad emission line has been observed and is believed to originate from gas rotating close to the central mass at a speed comparable to the speed of light [125],[33]. It has been claimed that the Kerr rotation parameter of the postulated black hole in MCG-6-30-15 can be constrained to a value close to unity [23], though this has since been challenged [114].

2.4. BETTER EVIDENCE ?

Due to the nature of a black hole, it is difficult to prove its existence directly. Arguably, the best proof would be based on strong field general relativistic effects. However, quite generally, these effects can be well imitated by a neutron star or a more exotic compact object with a radius of a few Schwarzschild radii. The exception is the event horizon, which cannot be mimicked by any other object, since it is constitutive of black holes. Advection-dominated accretion flows may provide unique evidence for this intrinsic feature of black holes [96],[91],[88],[92].

3. Accretion solutions

3.1. WHY ACCRETION ?

Astrophysics deals with a variety of sources that show either persistent or intermittent high energy (typically X-ray) emission. Many of these sources involve enormous amounts of released energy. Accretion onto a neutron star or a black hole is the most efficient known process for converting matter into energy (excluding the obvious matter-antimatter annihilation process), far more efficient than the fusion of hydrogen into helium [38],[134]. Therefore, one is naturally inclined to explain high-energy astrophysical observations through the accretion paradigm.

In these models, the accreting gas radiates (in part or totally) the energy that it acquires in falling into the gravitational potential well of the central object. For a given accretion rate \dot{M} (quantity of matter per unit time), the gravitational energy available during accretion onto a spherical object of radius R_X and mass M_X is

$$L_{acc} = \frac{GM_X\dot{M}}{R_X}, \quad (2)$$

where G is the gravitational constant. The radiative efficiency of an accretion flow is defined as its ability to convert the rest mass of particles at infinity into radiated energy,

$$\eta = \frac{L_{rad}}{\dot{M}c^2}, \quad (3)$$

where L_{rad} is the luminosity radiated by the flow (less than L_{acc}) and c is the speed of light. For a compact object, i.e. an object with a large ratio M_X/R_X , we see from Eq. 2 that the efficiency is potentially very high. For a neutron star or a black hole, η can be ~ 0.1 (in contrast to the ~ 0.007 efficiency of hydrogen fusion).

It is convenient to scale the luminosity and the mass accretion rate in terms of the so-called Eddington limit. The Eddington luminosity is that luminosity at which the radiation pressure on a spherical flow balances the gravitational attraction of the central object:

$$L_{Edd} = 1.3 \times 10^{38} \left(\frac{M_X}{M_\odot} \right) \text{ erg s}^{-1}. \quad (4)$$

This is the theoretical upper limit to the luminosity of a steady spherical accretion flow (but it is usually meaningful for other geometrical configurations as well). Another useful quantity is the Eddington accretion rate, defined here as the accretion rate at which a 0.1 efficiency accretion flow emits the Eddington luminosity:

$$\dot{M}_{Edd} = \frac{L_{Edd}}{0.1c^2} = 1.4 \times 10^{18} \left(\frac{M_X}{M_\odot} \right) \text{ g s}^{-1}. \quad (5)$$

We use the following notation for the scaled accretion rate:

$$\dot{m} = \frac{\dot{M}}{\dot{M}_{Edd}}. \quad (6)$$

3.2. STANDARD SOLUTIONS

The equations describing the accretion of gas onto a central object are the standard conservation laws of mass, momentum and energy, coupled with detailed equations for the microscopic radiation processes. These equations are highly nonlinear, and allow multiple solutions. One is generally interested only in sufficiently stable solutions, since these are the ones that can be observed in nature.

Historically, the first solution to be considered was Bondi spherical accretion [11], in which matter without angular momentum accretes radially onto the central object. This solution is usually not relevant close to the central object (where the bulk of the observed radiation originates), since accreting matter in astrophysical settings invariably possesses a finite amount of angular momentum and cannot adopt a purely radial accretion configuration.

The second well known accretion solution is the “thin disk” solution in which matter revolves around the central object in nearly Keplerian orbits as it slowly accretes radially [121],[99],[108]. To reach the central object, the accreting matter must get rid of its angular momentum through viscous transport processes. Associated with the transport of angular momentum, viscous dissipation heats the accreting gas, and controls, along with

the cooling processes, the energetics of the accretion flow. In the thin disk solution, the viscously dissipated gravitational energy is radiated very efficiently. In terms of the efficiency defined in Eq. 3, a thin disk has $\eta \sim 0.06$ for a Schwarzschild black hole, and $\eta \sim 0.42$ for a maximally rotating Kerr black hole [26]. (In the case of a neutron star, $\eta \sim 0.2$.) Since the matter cools efficiently, it adopts a vertically thin configuration where $H/R \ll 1$, R being the distance from the central object and H the height of the disk as measured from the orbital plane. The thin disk solution has been the common paradigm in accretion theory for many years, and has been successfully applied to disks around young stars, disks in binaries and AGN disks [38].

The thin disk model assumes that, in steady-state (constant \dot{m} through the disk), the local viscous dissipation rate is everywhere exactly balanced by the locally emitted flux. The disk is optically thick, which means that each annulus of the disk emits a blackbody spectrum (to first approximation). The overall emission from the disk is the superposition of the emission from all annuli, which means a superposition of blackbody spectra at different temperatures. However, since the emission is dominated by the innermost annuli, what emerges is similar to a single temperature blackbody spectrum. For a detailed review of thin accretion disk theory and its applications, see *Accretion Power in Astrophysics* [38].

The thin disk model has serious difficulties explaining the properties of some observed systems. In particular, it cannot account for the fact that radiation from many systems often spans the entire electromagnetic spectrum, with significant emission from radio to gamma rays; this is very different from a simple blackbody type spectrum.

3.3. ADVECTION-DOMINATED ACCRETION FLOWS

The thin disk paradigm describes the structure of an accretion flow when the gas can (locally) radiate all of the viscously generated energy. When the gas does not radiate efficiently, the viscously generated energy is stored as thermal energy and advected by the flow. In this case, one has an ADAF, whose structure and properties are markedly different from a thin disk.

ADAFs can exist in two regimes. The first is when the gas is optically thin and the cooling time exceeds the inflow time (defined as the time-scale for matter to reach the central object) [56],[111],[94],[96],[1]. The second is when the gas is so optically thick that a typical photon diffusion time out of the flow exceeds the inflow time [60],[9],[3]. In both situations, the accretion flow is unable to cool efficiently and advects a significant fraction of the internally dissipated energy [18]. We focus on optically thin ADAFs, since they have seen the most applications to observed systems (see Narayan

[87] and Narayan, Mahadevan & Quataert [93] for reviews of ADAFs and their applications).

3.3.1. *Optically thin, two-temperature ADAFs: Basic Assumptions*

Important studies of two-temperature accretion flows and advection-dominated accretion flows have been carried out in the past [122],[56],[111], but a detailed and consistent picture has only emerged recently [94],[95],[96],[1], offering the opportunity to apply specific models to astrophysical systems.

A standard assumption in the theory of hot accretion flows is that the gas is two temperature, with the ions significantly hotter than the electrons. In two-temperature ADAFs (2-T ADAFs), the viscous dissipation is assumed to preferentially heat the ions. The fraction of the viscous heating that goes directly to the electrons is parameterized by a factor δ , usually set to 10^{-3} ($\sim m_e/m_p$). In addition, the electrons receive energy from the ions via Coulomb collisions. When the density is low, however, this process is not very efficient. Therefore, only a small fraction of the viscous energy reaches the electrons; this energy is usually radiated (though not always [84],[75]). The rest of the energy remains in the ions, which are unable to cool in an inflow time. The energy in the ions is thus advected with the flow and is finally deposited on the central object. If the object is a black hole, the energy disappears; if it has a surface, the advected energy is re-radiated.

The efficiency of the turbulent viscous transport and dissipation in the flow are parameterized, as in the standard thin disk theory, by the “ α -prescription” [121]: the viscosity is written as $\nu = \alpha c_s^2 / \Omega_K$, where α is the viscosity parameter, c_s is the sound speed in the plasma and Ω_K is the local Keplerian angular velocity. If we assume that the Balbus-Hawley instability [6] is the origin of the MHD turbulence in the flow, we expect the magnetic fields and the gas in an ADAF to be in equipartition (i.e. magnetic pressure comparable to gas pressure), and the viscosity parameter α to be close to 0.3 [55].

3.3.2. *2-T ADAFs: Properties of the Flow and the Emitted Radiation*

The dynamical properties of ADAFs were first described by analytical self-similar solutions [94]; these were soon replaced by global numerical solutions [2],[90],[19],[40],[107],[105]. The flows are geometrically thick ($H/R \sim 1$) and are well approximated as spherical flows with most of the gas properties roughly constant on spherical shells [95]. Matter falls onto the central object at radial speeds less than, but comparable to, the free fall velocity and with angular velocities significantly less than the local Keplerian value. ADAFs are radially convectively unstable, but the implications of this for the structure and dynamics of the flows are still unclear [96].

A self-consistent determination of the thermal structure of an ADAF

requires detailed numerical calculations [96],[88]. The poor energetic coupling between ions and electrons, and the advection of heat by the ions, is reflected in their temperature profiles: the ion temperature goes as $T_i \sim 10^{12} K/r$ (r is the distance from the central object in units of the Schwarzschild radius) while the electron temperature saturates at $T_e \sim 10^9-10^{10}$ K in the inner $10^2 - 10^3$ Schwarzschild radii. Above a critical accretion rate, \dot{m}_{crit} , the density in the plasma becomes sufficiently high that Coulomb collisions efficiently transfer energy from the ions to the electrons. The gas then radiates most of the viscously dissipated energy and is no longer advection-dominated. ADAFs therefore only exist for accretion rates below $\dot{m}_{crit} \sim \alpha^2$ [56],[111],[96],[1]. For $\dot{m} > \dot{m}_{crit}$, accretion occurs as a cool thin disk.

Since ADAFs are optically thin and most of the viscously released energy is advected, they are significantly underluminous compared to a thin accretion disk with the same accretion rate; in fact, the radiative efficiency can be as low as $\eta \sim 10^{-3} - 10^{-4}$ at low \dot{m} . The emission by the hot plasma comes almost entirely from the electrons. Bremsstrahlung is an important emission process. In addition, since the electrons are in the presence of significant magnetic fields and are marginally relativistic, synchrotron emission and inverse Compton radiation are also very important. Synchrotron emission is the dominant mechanism at radio, infrared and optical wavelengths, with the peak emission occurring at a wavelength that depends on the black hole mass ($\lambda_{peak} \propto M_X^{1/2}$) [73]. Comptonization of soft photons by hot electrons contributes from infrared to hard X-rays and is a strong function of the accretion rate. Bremsstrahlung emission generally dominates in the X-ray band at low mass accretion rates, but Comptonization takes over at higher accretion rates. A significant amount of γ -rays is also emitted, resulting from neutral pions (created by proton-proton collisions) which decay into very hard photons [74]. Pair creation processes are not very important in ADAFs since the radiation energy densities in the flow are low [12],[67].

3.3.3. 2-T ADAFs : Stability

The stability of accretion solutions is an important issue in accretion physics, since an accretion solution is not viable if it is unstable (by that one generally means linearly unstable). For instance, the important 2-T (non advective) solution of Shapiro et al. [122] is known to be violently unstable [106] and for this reason will probably never be observed in nature. The stability of 2-T ADAF solutions has been investigated in the long and short wavelength limits [96],[76],[59],[129],[130]. These studies conclude that, since the only unstable modes have sufficiently slow growth rates, ADAFs constitute a viable solution.

4. Applications of ADAFs

ADAF models have been applied to a number of low luminosity systems. They give a satisfying description of the spectral characteristics of the source Sgr A* at the center of our Milky Way Galaxy [92],[77], the weak AGN NGC 4258 [69] and M87 [115], and of several quiescent black hole XRBs [91],[88],[49]. All of these systems are known to experience low efficiency accretion and the thin disk solution encounters serious difficulties in explaining the observed spectral properties. In addition, the ADAF model also fits brighter systems with higher efficiencies [86],[30],[29].

It is worth mentioning here that previous studies have shown that the spectra of some of these systems can be explained by constructing models of optically thin accreting plasmas. However, these models are not necessarily dynamically consistent and do not explicitly attempt to satisfy mass, angular momentum and energy conservation. The ADAF solutions solve the observational and theoretical problems, for the first time, in a reliable and dynamically consistent way.

4.1. MODELING TECHNIQUES

Popham & Gammie [107], among others [2],[105], have computed the steady-state dynamical structure of ADAFs in the Kerr geometry. Their numerical solutions have been used in the spectral models presented here. The dynamical model provides the radial profiles of quantities such as radial speed, angular speed, density, pressure and viscous dissipation. In these models, the structure is determined by 3 parameters : α (viscosity parameter), γ (adiabatic index of the gas), and f (advection parameter, i.e. the fraction of the viscously dissipated energy which is advected). Usually, models assume that a constant fraction $(1 - \beta) = 0.5$ of the total pressure comes from the magnetic field pressure and that $\alpha \sim 0.6(1 - \beta) = 0.3$. The adiabatic index is given by $\gamma = (8 - 3\beta)/(6 - 3\beta) = 1.44$ [28]. The parameter f is solved self-consistently by calculating the radiation processes in detail and feeding back the information to the dynamical solution [30]. So far, studies have been restricted to the Schwarzschild geometry, but ultimately, in full generality, the Kerr rotation parameter a of the black hole will constitute an additional parameter.

The steady-state energetic structure of the flow is found by solving the electron and proton energy equations. The emission spectrum is obtained as a byproduct of this procedure, in which synchrotron, bremsstrahlung and Compton processes are all taken into account. Since soft photons can be scattered off electrons more than once before escaping the flow, the Compton problem has to be solved by a global “iterative scattering method” for consistency [88]. In the models presented here, the photon transport

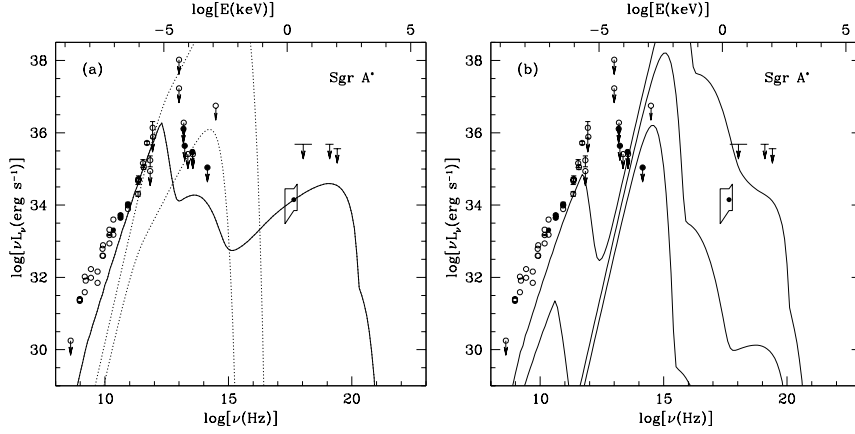


Figure 1. (a) Spectrum of an ADAF model of Sgr A* (solid line, based on [92]). The mass accretion rate inferred from this model is $\dot{m} = 1.3 \times 10^{-4}$ in Eddington units, in agreement with an independent observational determination. Dotted lines show the spectra of thin accretion disks, at the same accretion rate (upper) and at $\dot{m} = 1 \times 10^{-8}$ (lower). Observational data are shown as circles with error bars, and upper limits are indicated by arrows. The box indicates the constraints on the flux and the spectral index in soft X-rays. (b) Spectra of ADAF models of Sgr A* where the central mass is taken to have a surface at $3 R_{\text{Schw}}$ and the advected energy is assumed to be re-radiated as a blackbody. From top to bottom, the three spectra correspond to $\dot{m} = 10^{-4}, 10^{-6}, 10^{-8}$. All three models violate the infrared limit.

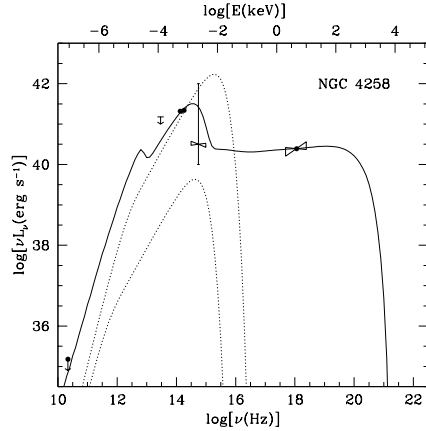


Figure 2. Spectrum of an ADAF model of NGC 4258 (solid line), at an accretion rate $\dot{m} = 9 \times 10^{-3}$, with a transition radius $R_{\text{trans}} = 30 R_{\text{Schw}}$. Dotted lines show the spectra of thin accretion disks, at an accretion rate $\dot{m} = 4 \times 10^{-3}$ (upper, adjusted to fit the infrared points) and $\dot{m} = 10^{-5}$ (lower).

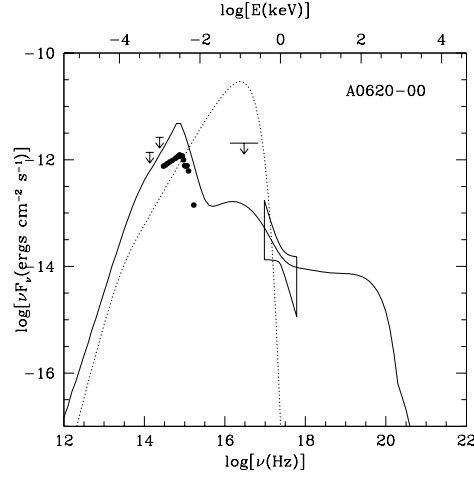


Figure 3. Spectrum of an ADAF model of A0620-00 (solid line, based on [88]) at an accretion rate $\dot{m} = 4 \times 10^{-4}$, compared with the observational data. The dotted line shows the spectrum of a thin accretion disk with an accretion rate $\dot{m} = 10^{-5}$ (adjusted to fit the optical flux).

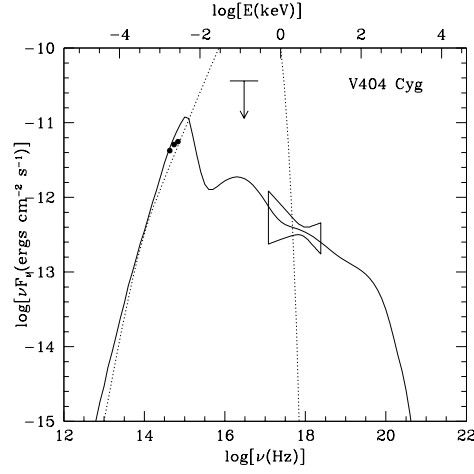


Figure 4. Spectrum of an ADAF model of V404 Cyg (solid line, based on ref. [88]) at an accretion rate $\dot{m} = 2 \times 10^{-3}$, compared with the observational data. The dotted line shows the spectrum of a thin accretion disk with $\dot{m} = 1.8 \times 10^{-3}$ (adjusted to fit the optical flux).

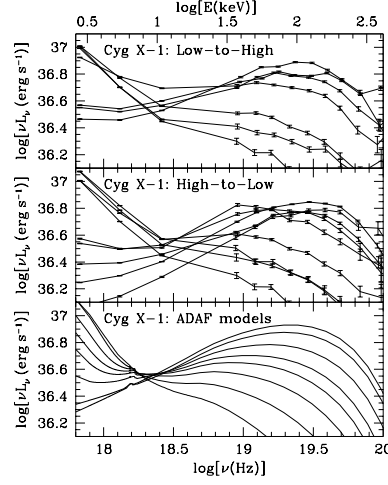


Figure 5. The broadband simultaneous RXTE (1.3-12 keV) and BATSE (20-600 keV) spectra of Cyg X-1 observed during the 1996 low-high (upper panel) and high-low (middle panel) state transitions. The bottom panel shows a sequence of ADAF models which are in good agreement with the observations [29].

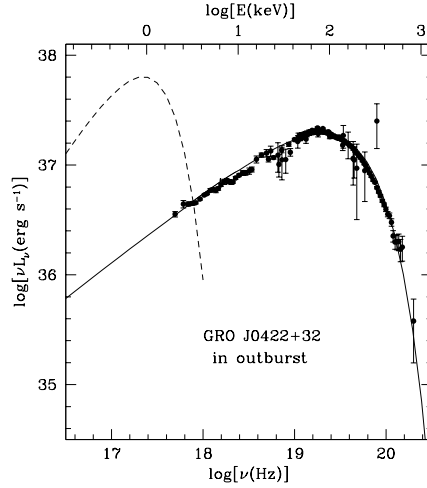


Figure 6. An ADAF model of J0422+32 (solid line) in the so-called low state (which is actually during outburst), compared with the observational data (dots and errorbars) [29]. The dashed line shows a thin disk model at the same accretion rate $\dot{m} = 0.1$.

has been treated as Newtonian, but including gravitational redshift effects. Generic ADAF spectra with photon transport in the Kerr metric have been computed by Jaroszynski & Kurpiewski [57].

The basic ADAF model has one adjustable parameter: the mass accretion rate \dot{m} . The X-ray flux emitted by the ADAF is very sensitive to the density and therefore the accretion rate. For this reason, \dot{m} is usually adjusted so that the resulting spectrum fits the available X-ray data.

The spectral characteristics of some systems are better explained by mixed ADAF + thin disk models. The accretion proceeds via an ADAF in the inner regions of the accretion flow, and via a thin disk beyond a so-called transition radius (R_{trans}). The contribution of the thin disk to the overall spectrum is a strongly decreasing function of R_{trans} , so that R_{trans} is a relevant parameter (and therefore is well determined) only in those systems where the thin disk contribution to the emitted flux is significant (see NGC 4258 and Cyg X-1, for instance).

ADAF models and the corresponding observational data points and constraints are shown in Fig. 1 to Fig. 6 for a number of well-known black hole systems. Spectra of thin accretion disks are also shown. While the ADAF models are in qualitative agreement with the observations, the thin disk models are generally ruled out quite convincingly.

4.2. SPECTRAL MODELS OF LOW LUMINOSITY SYSTEMS

4.2.1. *Sgr A**

Sgr A* is an enigmatic radio source at the center of our Galaxy. Dynamical mass estimates show that a dark mass $M \sim 2.5 \times 10^6 M_\odot$ resides in a region of less than 0.1 pc in extension around this source [27],[50],[51]. Based on this, it is assumed that Sgr A* is a supermassive black hole. Observations of gas flows and stellar winds in its vicinity suggest that Sgr A* accretes matter at a rate in the range $\dot{M} \sim \text{a few} \times 10^{-6} - 10^{-4} M_\odot \text{ yr}^{-1}$ ($\dot{m} \sim 10^{-4} - 10^{-2}$) [44],[80]. A standard thin disk accreting with this \dot{m} at a typical efficiency $\eta \sim 0.1$ is far too luminous to account for the observed integrated flux. Such a model also disagrees with the observed shape of the spectrum and is ruled out (by orders of magnitude) by an upper limit on the Sgr A* flux in the near infrared (Fig. 1a).

The first suggestion that Sgr A* may be advecting a significant amount of energy was made by Rees [110], and the first ADAF spectral model of this source appeared in Narayan, Yi & Mahadevan [97]. Since then, the modeling techniques [85],[84] and observational constraints have improved, allowing the construction of a refined model of Sgr A* [92],[77]. The model is consistent with the *independent* estimates of M and \dot{M} mentioned above,

and it fits the observed fluxes in the radio, millimeter and X-ray bands and upper limits in the sub-millimeter and infrared bands (see Fig. 1a).

In evaluating the quality of the fit in Fig. 1a, it should be kept in mind that only one parameter, \dot{m} , has been adjusted; this parameter has been optimized to fit the X-ray flux at 2 keV. The position of the synchrotron peak at 10^{12} Hz and its amplitude are not fitted but are predicted by the model; the agreement with the data is good. There is, however, a problem at lower radio frequencies, $\leq 10^{10}$ Hz, where the model is well below the observed flux. This is currently unexplained.

An important feature of the ADAF model of Sgr A* is that the observed low luminosity of the source is explained as a natural consequence of the advection of energy in the flow (the radiative efficiency is very low, $\eta \sim 5 \times 10^{-6}$) and the disappearance of this energy through the event horizon of the black hole. The model will not work if the central object has a hard surface, as demonstrated in Fig. 1b.

4.2.2. NGC 4258

The mass of the central black hole in the AGN NGC 4258 has been measured to be $3.6 \times 10^7 M_\odot$ [83]. Highlighting the fact that the observed optical/UV and X-ray luminosities are significantly sub-Eddington ($\sim 10^{-4}$ and $\sim 10^{-5}$ respectively), Lasota et al. [69] proposed that accretion in NGC 4258 proceeds through an ADAF. They found that the emission spectrum and the low luminosity of this system can be explained by an ADAF model, provided that most of the viscously dissipated energy in the flow is advected into a central black hole. Since then, new infrared measurements have been made [17] that constrain the transition radius to be $R_{trans} \sim 30$ Schwarzschild radii. The ADAF produces the X-ray emission while the outer thin disk accounts for the newly observed infrared emission (see Fig. 2, unpublished). The refined model is also in agreement with a revised upper limit on the radio flux [109]. Maoz & McKee [78] and Kumar [66] find, via quite independent arguments, an accretion rate for NGC 4258 in agreement with the ADAF model. Neufeld & Maloney [98] estimate a much lower \dot{m} ($\leq 10^{-5}$) in order to explain the maser emission in the source, but it is hard to explain the observed spectrum with such an \dot{m} (Fig. 2).

4.2.3. Other Low Luminosity Galactic Nuclei

Quasars are luminous high redshift AGN, which are believed to be powered by supermassive black holes with masses around $10^8 - 10^9 M_\odot$ [112]. Most nearby bright elliptical galaxies are believed to host dead quasars, i.e. quasars which have become inactive through evolution [124],[21]. As pointed out by Fabian & Canizares [32], however, the nuclei of these elliptical galaxies are much too dim, given the mass accretion rates inferred

from independent methods. Fabian & Rees [34] suggested that the problem could be resolved if the accretion in these nuclei is occurring through an ADAF. This proposition has been confirmed by Mahadevan [73] and models have been developed for specific galaxies such as M87 [115] and M60 [24]. Lasota et al. [69] have similarly argued that low-luminosity LINER and Seyfert galaxies have supermassive black holes in their nuclei accreting via ADAFs.

4.2.4. *A0620-00 and V404 Cyg*

Soft X-ray Transients (SXTs) are a class of mass transfer X-ray binaries in which the accreting star is often a black hole candidate. Episodically, these systems enter high luminosity “outburst” phases, but for most of the time they remain in a very low luminosity “quiescent” phase. One of the main issues in modeling black hole SXTs in quiescence is that a thin accretion disk cannot explain both the observed low luminosity and the X-ray flux in these systems : at an accretion rate low enough to fit the observed luminosity, a thin disk will not emit any significant flux in the X-ray band. Moreover, the X-ray spectrum will have the wrong shape. Narayan, McClintock & Yi [91] argued that the dilemma can be solved by means of the ADAF model and demonstrated this by carrying out spectral fits of A0620-00, V404 Cyg and Nova Mus 91 in quiescence. Narayan, Barret & McClintock [88] have recently refined these models for V404 Cyg and A0620-00 (see Fig. 3 and Fig. 4). The models are in good agreement with the observed shapes of the X-ray spectra (recall that the X-ray flux level is fitted by adjusting \dot{m} , but the spectral slope is unconstrained in the fit) and they satisfy other observational constraints such as optical measurements and extreme ultraviolet upper limits. In the optical, the models are somewhat too luminous to fit the data; the shapes of the spectra, however, are predicted well (see especially Fig. 3, where the position of the peak is reproduced well by the model). In contrast, the thin disk model deviates very significantly from the data and is easily ruled out. Hameury et al. [49] showed that observations of another SXT, GRO J1655-40, are consistent with the presence of an ADAF in quiescence. In addition, their model provides a convincing explanation for the time delay that was observed between the optical and X-ray light curves during a recent outburst [104].

4.3. MORE LUMINOUS SYSTEMS

4.3.1. *Spectral States of XRBs*

Narayan [86] suggested that the various spectral states (from quiescence to the luminous outburst phase) of black hole binaries (especially SXTs) can be understood in terms of a sequence of thin disk + ADAF models, where

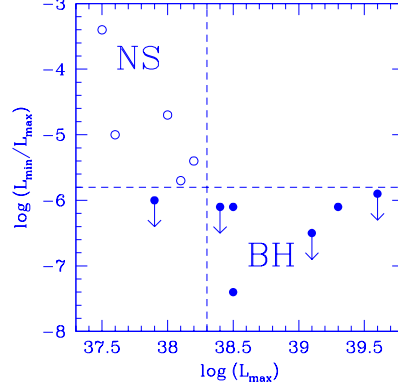


Figure 7. A comparison between black hole (BH, filled circles) and neutron star (NS, open circles) SXT luminosity variations [41]. The ratio of the quiescent luminosity to the peak outburst luminosity is systematically smaller for BH systems than for NS systems. This confirms the presence of event horizons in BH candidates.

the thin disk accounts for most of the luminosity in outburst and is gradually replaced by an ADAF during the transition to quiescence. Recently, Esin et al. [30] have developed these ideas with detailed calculations, and succeeded in explaining the observed spectral states of the system Nova Mus 91 surprisingly well. The same models also appear to explain other luminous black hole systems such as Cyg X-1 (Fig. 5) and J0422+32 (in outburst, Fig. 6) [29]. These studies, for the first time, unify a fair fraction of the phenomenology of black hole XRBs. Once again, the existence of a central black hole, into which energy is lost, is an essential feature of the models.

4.3.2. Galaxies and Quasars

A similar unification is also possible in our understanding of the various degrees of activity in galactic nuclei. Yi [131] has proposed an explanation for the apparent evolution of quasars from a large population of luminous objects at redshift ≥ 2 to a much smaller population in the nearby universe. He postulates that the mass accretion rate in galactic nuclei has decreased over cosmic time. Supermassive black holes in galactic nuclei had $\dot{m} > \dot{m}_{crit}$ at early times and accreted through thin disks with a high radiative

efficiency. As \dot{m} decreased with time, the accretion flow switched to a low efficiency ADAF. This explains the absence of very luminous AGN in the local neighborhood of our Galaxy.

Di Matteo & Fabian [25] proposed that a significant fraction of the hard X-ray (≥ 2 keV) background could be due to emission from a population of galaxies undergoing advection-dominated accretion in their nuclei. Yi & Boughn [132] discuss a test of the ADAF paradigm in this context; they argue that measurements of the radio and X-ray fluxes could provide direct estimates of the central black hole masses in many galaxies.

4.3.3. *Neutron Star SXTs vs. Black Hole SXTs*

As mentioned earlier, SXTs are XRBs that exhibit large luminosity variations. Most of the time they remain in a quiescent state, in which their luminosities are low and the transferred mass is partially stored in a non-steady thin disk. Episodically, they experience an outburst event, during which their luminosities become very high [68]. During outbursts, which correspond to a sudden accretion of the mass stored in the disk, these sources reach luminosities of order the Eddington luminosity (cf. Eq. 4). From dynamical mass estimates, and observations of “X-ray bursts” (very probably thermonuclear explosions on the surface of neutron stars), one can distinguish between neutron star and black hole candidate systems [135]. Since black holes are more massive than neutron stars (and the Eddington luminosity scales with the mass of the accreting object), black hole SXTs are naturally observed in outburst at a higher maximum luminosity than neutron star SXTs.

Assuming that the ADAF model of SXTs in quiescence [91],[88] is generic, Narayan, Garcia & McClintock [89] argued that black hole SXTs should experience more substantial luminosity changes from quiescence to outburst than neutron star SXTs. In quiescence, the central object accretes matter through an ADAF : most of the viscously dissipated energy is advected by the flow onto the central object. In the neutron star case, this advected energy has to be re-radiated from the stellar surface, whereas in the black hole case, it is lost through the horizon. Therefore, black hole SXTs in quiescence must be much less luminous (relative to their maximum luminosity) than neutron star SXTs, which is exactly what is observed in nature (see Fig. 7). This systematic effect confirms the presence of an event horizon in black hole SXTs [89],[41].

5. Conclusion

Advection-dominated accretion flow models of black holes in various XRBs and AGN are in qualitative agreement with the best current observations.

They provide a satisfying explanation for both the spectral characteristics and the extremely low luminosities observed in these systems. The models require that a very large fraction of the dissipated energy in the flow is advected into the central black hole. If a standard star with a surface, and not an event horizon, were present at the center of these systems, changes in the spectra and luminosities by orders of magnitude are predicted (e.g. compare Fig. 1a and Fig. 1b). The success of ADAF models thus constitutes strong evidence for the existence of stellar mass and supermassive black holes in the Universe.

We conclude with an interesting observation. If one considers the candidate black hole XRBs listed in Table 1, apart from LMC X-3, all the other systems spend the bulk of their time in the ADAF state and only occasionally switch to the more efficient thin accretion disk state. Similarly, in Table 2, the three best candidates, Sgr A*, NGC 4258 and M87, appear to have ADAFs, and it is plausible that many of the other systems have ADAFs as well, except for NGC 1068, MCG-6-30-15, and possibly NGC 4945. If ADAFs are, as the evidence suggests, very common, there is in principle no difficulty finding systems in which to test for the presence of event horizons. The challenge at the moment is primarily observational — ADAFs by their nature are very dim and one needs instruments with superior sensitivity to achieve adequate signal-to-noise.

Acknowledgments

We are grateful to Vicky Kalogera, Chris Kochanek, Avi Loeb, Rohan Mahadevan, Jeff McClintock and Doug Richstone for useful discussions. Fig. 5 and Fig. 6 were kindly provided by Ann Esin. The electronic preprints referenced below can be found at the Los Alamos National Laboratory e-print service : <http://xxx.lanl.gov/>. This work was supported in part by NSF grant AST 9423209 and NASA grant NAG 5-2837. EQ was supported by a NSF graduate research fellowship.

References

1. Abramowicz, M.A., et al. (1995), *Astrop. J. Lett.* **438**, L37.
2. Abramowicz, M.A., Chen, X.-M., Granath, M., and Lasota, J.-P. (1996), *Astrop. J.* **471**, 762.
3. Abramowicz, M.A., Czerny, B., Lasota, J.-P., and Szuszkiewicz, E. (1988), *Astrop. J.* **332**, 646.
4. Bahcall, S., Lynn, B.W., and Selipsky, S.B. (1990), *Astrop. J.* **362**, 251.
5. Bailyn, C.D. et al. (1995), *Nature* **378**, 157.
6. Balbus, S.A., and Hawley, J.H. (1991), *Astrop. J.* **376**, 214.
7. Beekman, G., et al. (1997), *Mon. Not. R. Astron. Soc.* **290**, 303.
8. Bender, R., Kormendy, J., and Dehnen, W. (1996), *Astrop. J. Lett.* **464**, L123.
9. Begelman, M.C. (1978), *Mon. Not. R. Astron. Soc.* **184**, 53.

10. Binney, J., and Tremaine, S. (1987), *Galactic Dynamics* (Princeton University Press, Princeton).
11. Bondi, H. (1952), *Mon. Not. R. Astron. Soc.* **112**, 195.
12. Bjornsson, G., Abramowicz, M.A., Chen, X.-M., and Lasota, J.-P. (1996), *Astrop. J.* **467**, 99.
13. Bower, G.A., et al. (1997), *Astrop. J. Lett.* in press, *Astro-ph/9710264*.
14. Callanan, P.J. et al. (1996), *Astrop. J. Lett.* **470**, L57.
15. Casares, J., et al. (1995), *Mon. Not. R. Astron. Soc.* **276**, L35.
16. Chandrasekhar, S. (1931), *Mon. Not. R. Astron. Soc.* **91**, 456.
17. Chary, R., and Becklin, E.E. (1997), *Astrop. J. Lett.* **485**, L75.
18. Chen, X., et al., (1995), *Astrop. J. Lett.* **443**, L61.
19. Chen, X., Abramowicz, M.A., and Lasota, J.-P. (1997), *Astrop. J.* **476**, 61.
20. Chen, W., Shrader, C.R., and Livio, M. (1997), *Astrop. J.* in press, *Astro-ph/9707138*.
21. Chokshi, A., and Turner, E.L. (1992), *Mon. Not. R. Astron. Soc.* **259**, 421.
22. Cowley, A.P. et al. (1983), *Astrop. J.* **272**, 118.
23. Dabrowski, Y., et al. (1997), *Mon. Not. R. Astron. Soc.* **288**, L11.
24. Di Matteo, T., and Fabian, A.C. (1997), *Mon. Not. R. Astron. Soc.* **286**, 50.
25. Di Matteo, T., and Fabian, A.C. (1997), *Mon. Not. R. Astron. Soc.* **286**, 393.
26. Eardley, D.M. and Press, W.H. (1975), *Annu. Rev. Astron. Astrop.* **13**, 381.
27. Eckart, A., and Genzel, R. (1997), *Mon. Not. R. Astron. Soc.* **284**, 576.
28. Esin, A.A. (1997), *Astrop. J.* **482**, 400.
29. Esin, A.A., et al. (1997), *Astrop. J.* submitted, *Astro-ph/9711167*.
30. Esin, A.A., McClintock, J.E., and Narayan, R. (1997), *Astrop. J.* **489**, 865.
31. Esin, A.A., Narayan, R., Ostriker, E., and Yi, I. (1996), *Astrop. J.* **465**, 312.
32. Fabian, A.C., and Canizares, C.R. (1988), *Nature* **333**, 829.
33. Fabian, A.C., et al. (1995), *Mon. Not. R. Astron. Soc.* **277**, L11.
34. Fabian, A.C., and Rees, M.J. (1995), *Mon. Not. R. Astron. Soc.* **277**, L55.
35. Ferrarese, L., Ford, H.C., and Jaffe, W. (1996), *Astrop. J.* **470**, 444.
36. Filippenko, A.V., Matheson, T., and Ho, L.C. (1995), *Astrop. J.* **455**, 614.
37. Ford, H.C., Tsvetanov, Z.I., Ferrarese, L., and Jaffe, W. (1997), in proc. IAU Symp. 184, *The Central Region of the Galaxy and Galaxies*, ed. Y. Sofue, *Astro-ph/9711299*.
38. Frank, J., King, A., and Raine, D. (1992), *Accretion Power in Astrophysics*, 2nd Ed. (Cambridge University Press, Cambridge).
39. Friedman, J.L., and Ipser, J.R. (1987), *Astrop. J.* **314**, 594.
40. Gammie, C.F., and Popham, R. (1997), *Astrop. J.* submitted, *Astro-ph/9705117*.
41. Garcia, M.R., McClintock, J.E., Narayan, R., and Callanan, P.J. (1997), in Proc. 13th NAW on CVs, Jackson Hole, eds S. Howell, E. Kuulkers, and C. Woodward, *Astro-ph/9708149*.
42. Gebhardt, K., et al. (1996), *Bull. Am. Astron. Soc.* **28**, 1422.
43. George, I.M. and Fabian, A.C. (1991), *Mon. Not. R. Astron. Soc.* **249**, 352.
44. Genzel, R., Hollenbach, D., and Townes, C.H. (1994), *Rep. Prog. Phys.* **57**, 417.
45. Genzel, R., Eckart, A., Ott, T., and Eisenhauer, F. (1997), *Mon. Not. R. Astron. Soc.* **291**, 219.
46. Gies, D.R., and Bolton, C.T. (1982), *Astrop. J.* **260**, 240.
47. Greenhill, L.J., Gwinn, C.R., Antonucci, R., and Barvainis, R. (1996), *Astrop. J. Lett.* **472**, L21.
48. Greenhill, L.J., Moran, J.M., and Herrnstein, J.R. (1997), *Astrop. J. Lett.* **481**, L23.
49. Hameury, J.-M., Lasota, J.-P., McClintock, J.E., and Narayan, R. (1997), *Astrop. J.* in press, *Astro-ph/9703095*.
50. Haller, J.-W., et al. (1996), *Astrop. J.* **456**, 194.
51. Haller, J.-W., et al. (1996), *Astrop. J.* **468**, 955.
52. Harms, R.J., et al. (1994), *Astrop. J. Lett.* **435**, L35.

53. Hartle, J.B. (1978), *Phys. Rep.* **46**, 201.
54. Hartle, J.B. and Sabbadini, A.G. (1977), *Astrop. J.* **213**, 831.
55. Hawley, J.F., Gammie, C.F., and Balbus, S.A. (1996), *Astrop. J.* **464**, 690.
56. Ichimaru, S. (1977), *Astrop. J.* **214**, 840.
57. Jaroszynski, M., and Kurpiewski, A. (1997), *Astron. Astrop.* **326**, 419.
58. Kalogera, V. and Baym, G. (1996), *Astrop. J. Lett.* **470**, L61.
59. Kato, S., Yamasaki, T., Abramowicz, M.A., and Chen, X.-M. (1997), *Publ. Astron. Soc. Jap.*, **49**, 221.
60. Katz, J. (1977), *Astrop. J.* **215**, 265.
61. Kerr, R.P. (1963), *Phys. Rev. Lett.* **11**, 237.
62. Kormendy, J., et al. (1996), *Astrop. J. Lett.* **459**, L57.
63. Kormendy, J., et al. (1996), *Astrop. J. Lett.* **473**, L91.
64. Kormendy, J., et al. (1997), *Astrop. J.* in press, *Astro-ph/9703188*.
65. Kormendy, J., and Richstone, D. (1995), *Annu. Rev. Astron. Astrop.* **33**, 581.
66. Kumar, P. (1997), *Astrop. J.* submitted, *Astro-ph/9706063*.
67. Kusunose, M., and Mineshige, S. (1996), *Astrop. J.* **468**, 330.
68. Lasota, J.-P. (1996), in *Compact Stars in Binaries* (IAU), ed. J. van Paradijs et al.
69. Lasota, J.-P., et al. (1996), *Astrop. J.* **462**, 142.
70. Lynden-Bell, D. (1969), *Nature* **223**, 690.
71. Macchetto, F., et al. (1997), *Astrop. J.* **489**, 579.
72. McClintock, J.E., and Remillard, R.A. (1986), *Astrop. J.* **308**, 110.
73. Mahadevan, R. (1997), *Astrop. J.* **477**, 585.
74. Mahadevan, R., Narayan, R., and Krolik, J. (1997), *Astrop. J.* **486**, 268.
75. Mahadevan, R., and Quataert, E. (1997), *Astrop. J.* **490**, 605.
76. Manmoto, T., et al. (1996), *Astrop. J. Lett.* **464**, L135.
77. Manmoto, T., Mineshige, S., and Kusunose, M. (1997), *Astrop. J.* **489**, 791.
78. Maoz, E. and McKee, C.F. *Astrop. J.* in press, *Astro-ph/9704050* (1997).
79. Matt, G., Fabian, A.C. and Reynolds, C.S. (1997), *Mon. Not. R. Astron. Soc.* **289**, 175.
80. Melia, F. (1992), *Astrop. J. Lett.* **387**, L25.
81. Miller, J.C., Shahbaz, T. and Nolan, L.A. (1997), *Mon. Not. R. Astron. Soc.* submitted, *Astro-ph/9708065*.
82. Misner, C.W., Thorne, K.S., and Wheeler, J.A. (1973), *Gravitation* (Freeman and Co., New York).
83. Miyoshi, M., et al. (1995), *Nature* **373**, 127.
84. Nakamura, K.E., Kusunose, M., Matsumoto, R., and Kato, S. (1997), *Publ. Astron. Soc. Jap.*, **49**, 503.
85. Nakamura, K.E., Matsumoto, R., Kusunose, M., and Kato, S. (1996), *Publ. Astron. Soc. Jap.*, **48**, 761.
86. Narayan, R. (1996), *Astrop. J.* **462**, 136.
87. Narayan, R. (1997), in Proc. IAU Colloq. 163, ASP Conf. Series vol. 121, *Accretion Phenomena and Related Outflows*, eds. D. T. Wickramasinghe, L. Ferrario and G. V. Bicknell, p. 75.
88. Narayan, R., Barret, D., and McClintock, J.E. (1997), *Astrop. J.* **482**, 448.
89. Narayan, R., Garcia, M.R., and McClintock, J.E. (1997), *Astrop. J. Lett.* **478**, L79.
90. Narayan, R., Kato, S., and Honma, F. (1997), *Astrop. J.* **476**, 49.
91. Narayan, R., McClintock, J.E., and Yi, I. (1996), *Astrop. J.* **457**, 821.
92. Narayan, R., et al. (1997), *Astrop. J.* in press, *Astro-ph/9706112*.
93. Narayan, R., Mahadevan, R., and Quataert, E. (1998), in *The Theory of Black Hole Accretion Discs*, eds. M. A. Abramowicz, G. Bjornsson and J. E. Pringle, in press, *Astro-ph/9803141*.
94. Narayan, R., and Yi, I. (1994), *Astrop. J. Lett.* **428**, L13.
95. Narayan, R., and Yi, I. (1995), *Astrop. J.* **444**, 231.
96. Narayan, R., and Yi, I. (1995), *Astrop. J.* **452**, 710.

97. Narayan, R., Yi, I., and Mahadevan, R. (1995), *Nature* **374**, 623.
98. Neufeld, D.A., and Maloney, P.R. (1995), *Astrop. J. Lett.* **447**, L17.
99. Novikov, I.D., and Thorne, K.S. (1973), in *Blackholes*, ed. C. DeWitt and B. DeWitt (Gordon and Breach, New York).
100. Oppenheimer, J.R., and Snyder, H. (1939), *Phys. Rev.* **56**, 455.
101. Orosz, J.A., et al. (1996), *Astrop. J.* **468**, 380.
102. Orosz, J.A., and Bailyn, C.D. (1997), *Astrop. J.* **477**, 876.
103. Orosz, J.A., et al. (1997), *Astrop. J.* submitted.
104. Orosz, J.A., et al. (1997), *Astrop. J.* **478**, 830.
105. Peitz, J. and Appl, S. (1997), *Mon. Not. R. Astron. Soc.* **286**, 681.
106. Piran, T. (1978), *Astrop. J.* **221**, 652.
107. Popham, R. and Gammie, C.F. (1997), *Astrop. J.* submitted.
108. Pringle, J.E. (1981), *Annu. Rev. Astron. Astrop.* **19**, 137.
109. Herrnstein, J.R. et al. (1997), private communication.
110. Rees, M.J. (1982), in *The Galactic Center*, eds G. Riegler and R. D. Blandford.
111. Rees, M.J., Begelman, M.C., Blandford, R.D., and Phinney, E.S. (1982), *Nature* **295**, 17.
112. Rees, M.J. (1984), *Annu. Rev. Astron. Astrop.* **22**, 471.
113. Remillard, R.A. (1996), *Astrop. J.* **459**, 226.
114. Reynolds, C.S., and Begelman, M.C. (1997), *Astrop. J.* in press, *Astro-ph/9705136*.
115. Reynolds, C.S., et al. (1996), *Mon. Not. R. Astron. Soc.* **283**, L111.
116. Rhoades, C.E., and Ruffini, R. (1974), *Phys. Rev. Lett.* **32**, 6.
117. Richstone, D. (1997), in proc. IAU Symp. 184, *The Central Region of the Galaxy and Galaxies*, ed. Y. Sofue.
118. Sanwal, D., et al. (1996), *Astrop. J.* **460**, 437.
119. Shahbaz, T., et al. (1994), *Mon. Not. R. Astron. Soc.* **271**, L10.
120. Shahbaz, T., Naylor, T., and Charles, P.A. (1994), *Mon. Not. R. Astron. Soc.* **268**, 756.
121. Shakura, N.I., and Sunyaev, R.A. (1973), *Astron. Astrop.* **24**, 337.
122. Shapiro, S.L., Lightman, A.P., and Eardley, D.M. (1976), *Astrop. J.* **204**, 187.
123. Shapiro, S.L., and Teukolsky, S.A. (1983), *Blackholes, White Dwarfs and Neutron Stars*, (Wiley Interscience, New York).
124. Soltan, A. (1982), *Mon. Not. R. Astron. Soc.* **200**, 115.
125. Tanaka, Y., et al. (1995), *Nature* **375**, 659.
126. van der Marel, R.P., de Zeeuw, P.T., Rix, H.-W., and Quinlan, G.D. (1997), *Nature* **385**, 610.
127. van der Marel, R.P., Cretton, N., de Zeeuw, P.-T., and Rix, H.-W. (1997), *Astrop. J.* submitted, *Astro-ph/9705081*.
128. Wandel, A., and Mushotzky, R.F. (1986), *Astrop. J. Lett.* **306**, L61.
129. Wu, X.-B. (1997), *Astrop. J.* **489**, 222.
130. Wu, X.-B. (1997), *Mon. Not. R. Astron. Soc.* in press, *Astro-ph/9707329*.
131. Yi, I. (1996), *Astrop. J.* **473**, 645.
132. Yi, I., and Boughn, S.P. (1997), *Astrop. J.* submitted, *Astro-ph/9710147*.
133. Zhang, S.N., et al. (1997), in proc. 4th Compton Symposium, eds. C. D. Dermer and J. D. Kurfess, *Astro-ph/9707321*.
134. *Physics of Active Galactic Nuclei*, eds. W. J. Duschl and S. J. Wagner (1992), (Springer, Berlin).
135. *X-ray Binaries*, eds. W. H. G. Lewin, J. Van Paradijs and E. P. J. Van den Heuvel (1995), (Cambridge University Press, Cambridge).